

Multicomponent inverse scattering series internal multiple prediction in the τ -p domain

Jian Sun* and Kristopher A. Innanen, Dept. of Geoscience, CREWES Project, University of Calgary

SUMMARY

Internal multiples constitute unique signal in seismic records, which can negatively impact subsurface imaging and subsequent amplitude analysis, or, potentially, enhance illumination due to their distinct reflection angles and longer ray-paths. Both conventional migration using primaries only, and improved imaging approaches involving internal multiples, benefit from the precise identification and separation of internal multiples from primaries. Elastic versions of the inverse scattering series internal multiple attenuation algorithm extend prediction capacity to include wave-mode conversion and other elastic effects. In spite of having been published in the 1990s, however, little to no numerical analysis of multicomponent versions of the algorithm has been presented, possibly because of the difficulty of finding integral limits which completely suppress artifacts. We present a plane-wave (τ -p) formulation, which admits, possibly uniquely, a sufficiently aggressive limitation on integration limits to create artifact-free P-P and P-S predictions. The process is illustrated with 1.5D synthetic data.

INTRODUCTION

In seismic exploration, internal multiples are conventionally considered to be noise, with most seismic imaging algorithms dealing correctly only with primary reflections. One reason for this is that most migration and inversion methods are based on the Born approximation, i.e., the single scattering assumption. In the presence of a smooth and continuous velocity model, internal multiples lead to artificial, misleading, and false subsurface images (Berkhout and Verschuur, 2006; Behura et al, 2014; Li et al, 2016; Weglein, 2016). So, in practice, to maintain image quality, internal multiples are removed. It is worth noting that internal multiples are unique bearers of information, with smaller reflection angles and longer ray-path than primary events. These features of internal multiples recorded in seismic data in principle increase the aperture of illumination and enhance subsurface imaging and structure determination. Rather than eliminating internal multiples, as is done in conventional imaging processes, migration of internal multiples under appropriate imaging conditions could provide more stratigraphic information and illuminate shadow zones where primaries cannot reach (Malcolm et al., 2009; Liu et al., 2011; Slob et al., 2014), for example, in sub-salt areas. Whether they are to be removed or used, the ability to separate and identify them is very important.

Considerable progress in internal multiple prediction has been made recently. There are two main ways to predict internal multiples from primary events. One is by transforming internal multiples to be 'surface-related' and then eliminating them using modified surface methods (Kelamis et al. 2002; Berkhout and Verschuur 2005, 2006; Luo et al. 2007). The second, which occurs by considering internal multiples to be a combination of a certain sub-events based on the inverse scattering series, is fully automatic and tends to be optimal absent accurate subsurface information or known generators (Weglein et al. 1997; Zou and Weglein, 2013; Innanen, 2017). Prediction in the τ -p domain, because it is particularly robust to choice of the algorithm's integration limits, will likely play an especially important role in land application (Sun and Innanen 2015, 2016).

These approaches, though powerful, are based on the acoustic approximation, and so inverse scattering series prediction technology, as it is normally implemented, is inconsistent with multi-component acquisition in onshore and ocean-bottom environments. For the data-driven inverse scattering-based approach, wave-mode conversions in multi-component seismic records will impact the wavenumber/slowness-dependent relationships employed in the acoustic algorithm. Matson and Weglein (1996) and Matson (1997) presented an elastic inverse scattering series prediction algorithm incorporating multicomponent data and wave-mode conversions. However, the prediction algorithm, which involves calculations in the pseudo-depth domain, requires complex and precise elastic Stolt migrations to proceed, which may be one reason why no numerical examples or analysis of multicomponent predictions involving field data or full synthetics appears in the literature. Here we present a τ -p domain formulation of inverse scattering elastic multiple prediction. The main point of theoretical interest is that the vertical-time calculation requires an aggressive integral limit to avoid prediction artifacts related to wave-mode conversions. A 1.5D full-wave synthetic illustrates the features of the implementation.

THEORY

Standard elastic inverse scattering series algorithm

Matson (1997) showed that elastic internal multiples can be predicted by decomposing the inverse scattering series into P- and S-wave related modes, and building the scattering model around an isotropic elastic homogeneous background model. The algorithm is written:

Elastic internal multiple prediction

$$\begin{aligned}
& b_3^{ij} \left(k_{x_g}^i, k_{y_g}^i, k_{x_s}^j, k_{y_s}^j, \omega \right) \\
&= -\frac{1}{(2\pi)^2} \iiint_{-\infty}^{+\infty} dk_{x_1}^k dk_{y_1}^k dk_{x_2}^l dk_{y_2}^l e^{i v_1^k (z_s - z_g)} e^{-i v_2^l (z_s - z_g)} \\
&\quad \times \int_{-\infty}^{+\infty} dz_1 e^{i(v_1^k + v_1^l) z_1} b_1^{ik} \left(k_{x_g}^i, k_{y_g}^i, k_{x_1}^k, k_{y_1}^k, z_1 \right) \\
&\quad \times \int_{-\infty}^{z_1 - \epsilon} dz_2 e^{-i(v_2^l + v_2^k) z_2} b_1^{kl} \left(k_{x_1}^k, k_{y_1}^k, k_{x_2}^l, k_{y_2}^l, z_2 \right) \\
&\quad \times \int_{z_2 + \epsilon}^{+\infty} dz_3 e^{i(v_2^l + v_2^k) z_3} b_1^{lj} \left(k_{x_2}^l, k_{y_2}^l, k_{x_s}^j, k_{y_s}^j, z_3 \right)
\end{aligned} \quad (1)$$

where

$$v_M^l = \sqrt{\frac{\omega^2}{(c_0^l)^2} - (k_{x_M}^l)^2 - (k_{y_M}^l)^2} \quad (2)$$

with v_M^l being the vertical wavenumber associated with lateral wavenumbers $k_{x_M}^l$ and $k_{y_M}^l$, and isotropic-elastic-homogeneous reference velocities c_0^l , one for each wave mode, $I \in \{P, SH, SV\}$, and source/receiver location $M \in \{g, s\}$. The integration variables z_1, z_2, z_3 are in units of pseudo-depth, and satisfy the lower-higher-lower relationship $z_1 > z_2$ and $z_2 < z_3$. The input b_1^{ij} is a mode-decomposed and weighted version of measured seismic data related:

$$b_1^{ij} \left(k_{x_g}^i, k_{y_g}^i, k_{x_s}^j, k_{y_s}^j, z \right) = -i 2 v_g^j D^{ij} \left(k_{x_g}^i, k_{y_g}^i, k_{x_s}^j, k_{y_s}^j, z \right) \quad (3)$$

where $D^{ij} \left(k_{x_g}^i, k_{y_g}^i, k_{x_s}^j, k_{y_s}^j, z \right)$ are data associated with downgoing j -mode and upgoing i -mode with $i, j \in \{P, SH, SV\}$, mapped to pseudo-depth with an elastic Stolt migration.

By performing an inverse Fourier transform over the x - and y - wavenumber components related to the source-receiver locations, and frequency, the left-hand side of equation (1) becomes the set of predicted elastic internal multiples in the (x_g, y_g, x_s, y_s, t) domain (which may through adaptive subtraction be removed from the input data).

Adapted τ -p elastic algorithm

The monotonicity relationship between acoustic pseudo-depth and intercept, or vertical, time makes the transformation of the acoustic prediction algorithm to the τ -p domain straightforward. Elastic phenomena, such as wave-mode conversions, bring an element of complexity to the plane-wave elastic problem. Assuming a P-wave source, the two-way intercept times of PP- and PS-waves are related to pseudo-depth via

$$\begin{aligned}
\tau^{PP} &= 2\tau^P = \frac{2z \cos \theta_p}{\alpha} \\
\tau^{SP} &= \tau^P + \tau^S = z \left(\frac{\cos \theta_p}{\alpha} + \frac{\cos \theta_s}{\beta} \right)
\end{aligned} \quad (4)$$

where τ^P and τ^S are one-way intercept times for pure PP- and SS-waves, and α and β are the reference medium P- and S-waves velocities respectively. θ_p and θ_s are angles between downgoing/upgoing-waves and the vertical, for P- and S-wave separately. For layered cases, Snell's law enforces $k_{x_s}^P = k_{x_g}^P = k_{x_g}^{SV}$ for P-wave sources, and $k_{x_s}^{SV} = k_{x_g}^{SV} = k_{x_g}^P$ for S-wave sources. Assuming all sources and receivers are at the same depth (i.e., $z_s = z_g$), the elastic prediction algorithm in equation (1), re-formulated in the plane wave domain and reduced to 1.5D, is

$$\begin{aligned}
b_3^{ij} \left(p_g, \omega \right) &= -\frac{1}{(2\pi)^2} \int_{-\infty}^{+\infty} d\tau_1^{im} e^{i\omega\tau_1^{im}} b_1^{im} \left(p_g, \tau_1^{im} \right) \\
&\times \int_{-\infty}^{\Upsilon(\tau_1^{im}|\tau_2^{mn})-\epsilon} d\tau_2^{mn} e^{-i\omega\tau_2^{mn}} b_1^{mn} \left(p_g, \tau_2^{mn} \right) \int_{\Upsilon(\tau_2^{mn}|\tau_3^{nj})+\epsilon}^{+\infty} d\tau_3^{nj} e^{i\omega\tau_3^{nj}} b_1^{nj} \left(p_g, \tau_3^{nj} \right)
\end{aligned} \quad (5)$$

where

$$\Upsilon \left(\tau_X^{mn} | \tau_Y^{nj} \right) = \begin{cases} \tau_X^{mn}, & j=m; \\ \frac{\alpha+\beta}{2\beta} \tau_X^{mn}, & j=S \& m=P; \\ \frac{2\beta}{\alpha+\beta} \tau_X^{mn}, & j=P \& m=S. \end{cases} \quad (6)$$

However, prediction with this algorithm and/or with (1) present serious practical difficulties—selecting integration limits in which no artifacts arise does not appear to be possible. But, after some algebra, equation (5) can be rewritten as

$$\begin{aligned}
b_3^{ij} \left(p_g, \omega \right) &= -\frac{1}{(2\pi)^2} \int_{-\infty}^{+\infty} d\tau_2^{mn} e^{-i\omega\tau_2^{mn}} b_1^{mn} \left(p_g, \tau_2^{mn} \right) \\
&\times \int_{\Gamma(mn,im)\tau_2^{mn}+\epsilon}^{+\infty} d\tau_1^{im} e^{i\omega\tau_1^{im}} b_1^{im} \left(p_g, \tau_1^{im} \right) \int_{\Gamma(mn,nj)\tau_2^{mn}+\epsilon}^{+\infty} d\tau_3^{nj} e^{i\omega\tau_3^{nj}} b_1^{nj} \left(p_g, \tau_3^{nj} \right)
\end{aligned} \quad (7)$$

where

$$\Gamma(X, Y) = \begin{cases} \frac{\alpha}{\beta}, & X=SS; \\ \frac{\alpha+\beta}{2\beta}, & X \neq SS \& Y=PS/SP; \\ 1, & \text{others.} \end{cases} \quad (8)$$

Equation (7) is equivalent to equation (5), but it has the benefit of allowing a much more aggressive search parameter. Our analysis is suggestive that this form of the algorithm leads to a stable, and largely artifact-free, multicomponent prediction.

Elastic internal multiple prediction

NUMERICAL VALIDATION

A three-layer elastic model is built to create synthetic seismic records upon which the elastic multiple prediction formula (7) can be tested. The geological model and parameters are illustrated in Figure 1; from top to bottom, P-wave velocities are [2000, 3500, 2500] m/s, S-wave velocities are [1200, 2000, 1300] m/s, and densities are [1.5, 2.25, 1.6] g/cm³. A P-wave source is located at the centre surface of the model, and receivers at 4m intervals are arranged at same depth. With four absorbing boundaries (dashed line in the model shown in Figure 1), a multi-component shot gather is generated using a finite difference scheme (SOFI2D, Bohlen et al., 2012). The gather is plotted in Figure 2.

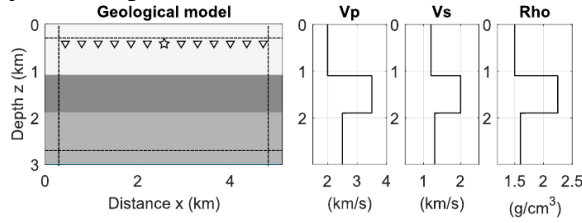


Figure 1: Geological model and parameters. Left panel: three layer model; right panel: P-,S-velocity and density profiles.

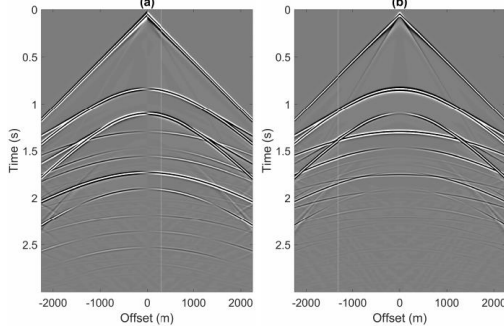


Figure 2: Multicomponent seismic records generated above the model in Figure 1. (a) Radial component; (b) vertical component.

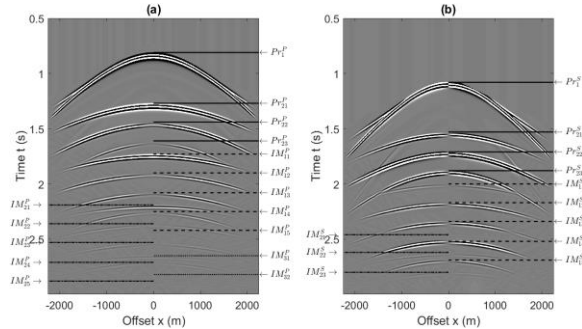


Figure 3: P- and S-wave decomposition of the data in Figure 2. (a) P-wave component; (b) SV-wave component. Pr denotes primary events, which are indicated by solid lines. IM denotes internal multiples. All events are enumerated in Table 1.

The direct arrivals are muted, after which the data are rotated into P- and S-wave components, as illustrated in Figure 3, with all reflection events labelled. The amplitude polarity is symmetric about zero offset in the P-wave component, and antisymmetric about zero-offset in the S-wave component. In the labeling system in Figure 3, for both P- and S-wave components, *Pr* denotes primaries, and *IM* represents internal multiples. Solid lines point to primary events. All 1st-order internal multiples are indicated with dashed lines, dashed-dotted lines label all 2nd-order internal multiples, and dotted lines label all 3rd-order internal multiples. The details of annotations for all reflection events are shown in Table 1.

Label-P	Primaries in P-mode	Label-S	Primaries S-mode
Pr_1^P	PP	Pr_1^S	PS
Pr_{21}^P	$PPPP$	Pr_{21}^S	$PPPS$
Pr_{22}^P	$PPSP$ & PSP	Pr_{22}^S	$PPSS$ & $PSPS$
Pr_{23}^P	$PSSP$	Pr_{23}^S	$PSSS$
Label-P	1st-order IMs in P-mode	Label-S	1st-order IMs in S-mode
IM_{11}^P	$\tilde{P}PPPP$	IM_{11}^S	$\tilde{P}PPPS$
IM_{12}^P	$\tilde{P}PPSP$	IM_{12}^S	$\tilde{P}PPSS$
IM_{13}^P	$\tilde{P}PPSSP$	IM_{13}^S	$\tilde{P}PPSSS$
IM_{14}^P	$\tilde{P}PSSSP$	IM_{14}^S	$\tilde{P}PSSSS$
IM_{15}^P	$\tilde{P}SSSSP$	IM_{15}^S	$\tilde{P}SSSSS$
Label-P	2nd-order IMs in P-mode	Label-S	2nd-order IMs in S-mode
IM_{21}^P	$\tilde{\tilde{P}}PPPPPP$	IM_{21}^S	$\tilde{\tilde{P}}PPPPPS$
IM_{22}^P	$\tilde{\tilde{P}}PPPPSP$	IM_{22}^S	$\tilde{\tilde{P}}PPPPSS$
IM_{23}^P	$\tilde{\tilde{P}}PPPPSSP$	IM_{23}^S	$\tilde{\tilde{P}}PPPPSSS$
IM_{24}^P	$\tilde{\tilde{P}}PPSSSSP$		
IM_{25}^P	$\tilde{\tilde{P}}PSSSSSP$		
Label-P	3rd-order IMs in P-mode		
IM_{31}^P	$\tilde{\tilde{\tilde{P}}}PPPPPPPP$		
IM_{32}^P	$\tilde{\tilde{\tilde{P}}}PPPPPPPS$		

Table 1: Symbols used in Figure 3.

In Table 1, the superscript indicates the wave-type. For primaries *Pr*, the first number of the subscript represents the corresponding generating reflector, and the second number is related to the number of S-wave travel-paths involved in the event. That is, it equals the number of S-wave ray-paths plus one in the P-wave mode, and the number of S-wave ray-paths directly in the S-wave mode. For internal multiples *IM*, the first number of the subscript is the order, and the second number is related to the number of S-wave ray-paths. The three inputs, b_1^{PP} , b_1^{SP} , and b_1^{PS} , for the plane-wave domain multicomponent prediction are computed through a weighted τ -p transform enacted on the P- and S-wave component data respectively:

$$\begin{aligned}
 b_1^{PP}(p, \omega) &= i2q^p D^{PP}(p, \omega) \\
 b_1^{SP}(p, \omega) &= i2q^p D^{SP}(p, \omega), \\
 b_1^{PS}(p, \omega) &= i2q^s D^{PS}(p, \omega)
 \end{aligned} \tag{9}$$

where $D^{PP}(p, \tau)$ and $D^{SP}(p, \tau)$ are the τ -p transformed, P-wave source data (Figure 4). $D^{PS}(p, \tau)$ has the same

Elastic internal multiple prediction

characteristics as $D^{SP}(p, \tau)$. All three fully-prepared inputs are illustrated in Figure 5.

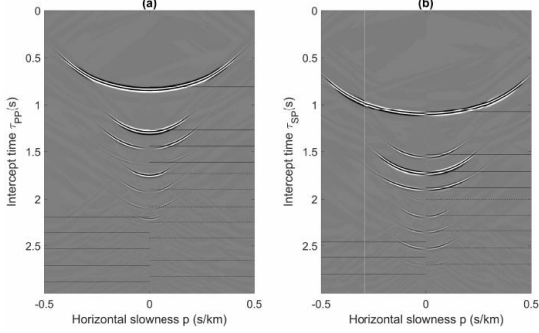


Figure 4: Plane wave / τ -p transformed, P-/S- decomposed data. (a) P-wave component; (b) SV-wave component.

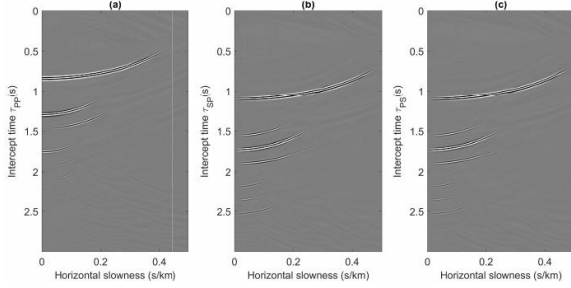


Figure 5: The 3 inputs to elastic prediction using the τ -p domain algorithm in equation (7); (a) input b_1^{PP} ; (b) input b_1^{SP} ; (c) input b_1^{PS} .

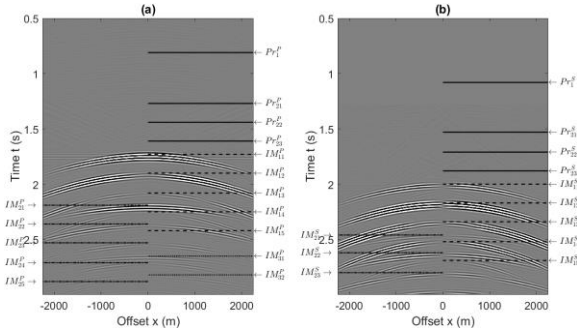


Figure 6: P-P and P-SV internal multiples predicted from the data in Figure 3 using formula (7). (a) P-P; (b) P-SV.

The elastic-multicomponent internal multiple prediction is computed by enacting formula (7) using this input, and then carrying out an inverse τ -p transform. The P- and S-wave components of the predicted multiples are plotted in Figure 6. To validate the predicted travel times of all internal multiples using ISS algorithm, same dotted / dashed / dot-dashed lines in Figure 3 and symbols in Table 1 are overlain in Figure 6 and compared with the predicted travel

times at zero-offset. Compared to the recorded data in Figure 3, no primary events or primary-related artifacts in the decomposed P-P and P-SV predictions are observed, and no expected multiples are missed by the prediction. Travel times of all elastic internal multiples are determined correctly both for P- and S-wave components. Waveform distortion is observed, but this is expected as no deconvolution was carried out on the input. Weak horizontal artifacts are observed at the zero offset travel times of the multiples which are tied to a non-sophisticated τ -p transform. Suppressing these with a high-resolution transform is a natural next step.

CONCLUSIONS

Internal multiple prediction is a high priority problem in seismic data processing, with special significance in unconventional plays where sophisticated quantitative interpretation of onshore multi-component data is apt to be applied. To take full advantage of the potential of data-driven inverse scattering series multiple prediction technology, we consider the numerical application of an elastic prediction theory dating from the 1990s. We are aware of no full numerical examples of the elastic prediction theory having been presented or analyzed in the literature. This may be because numerical implementation of multicomponent elastic inverse scattering multiple prediction is not straightforward. The mode-decomposed Stolt migrations must be combined in triplets, integrating over pseudo-depth, and the parameters limiting these integrations are difficult to select appropriately without introducing artifacts connected to mode-conversions. For this reason, and because of its other attractive features, we introduce a plane-wave/ τ -p formulation of the elastic prediction. This reformulation admits a much more aggressive integration-limiting scheme, which suppresses the conversion artifacts. The resulting algorithm is used to create 1.5D numerical predictions from synthetic data generated using an elastic finite-difference package (SOFI2D by *KIT Project*). A full accounting of all primaries and multiples in the input PP and PS records, matched up against the prediction, confirms the lack of artifacts and full capture of the wide range of multiple events. Waveform distortion and weak horizontal artifacts are connected to incomplete pre-processing and the features of the τ -p transform used respectively, and are the subject of ongoing refinements.

ACKNOWLEDGMENTS

The authors thank all sponsors of CREWES for their continued supports. We also thank Dr. Yu Geng and Hong Xu for useful discussions and suggestions. This work was funded by CREWES industrial sponsors and NSERC through the grant no. CRDPJ 461179-13.